2007

Fundamental-mode basin oscillations in the Japan/East Sea

Yongsheng Xu

D. Randolph Watts
University of Rhode Island, randywatts@uri.edu

See next page for additional authors

Citation/Publisher Attribution
Xu, Y., Watts, D. R., Wimbush, M., and Park, J.-H. (2007), Fundamental-mode basin oscillations in the Japan/East Sea, *Geophys. Res. Lett.*, 34, L04605, doi: 10.1029/2006GL028755.
Available at: https://doi.org/10.1029/2006GL028755

GEOPHYSICAL RESEARCH LETTERS, VOL. 34, L04605, doi:10.1029/2006GL028755, 2007

Fundamental-mode basin oscillations in the Japan/East Sea

Yongsheng Xu,[1,2] D. Randolph Watts,[2] Mark Wimbush,[2] and Jae-Hun Park[2]

Received 12 November 2006; revised 3 January 2007; accepted 19 January 2007; published 22 February 2007.

[1] We present observational evidence from coastal tide station and bottom pressure data that basin-mode oscillations are frequently excited in the Japan/East Sea (JES). The fundamental basin-mode is a Kelvin-wave-like oscillation consisting of a single amphidromic system around which the high water propagates counterclockwise. Its period is about 6.7 hours and its coastal wavelength is equivalent to the circumference of the JES. The relative amplitudes of the observed oscillations agree with Rikiishi's 1986 model results except for stations near the Korea Strait where the closed boundary in the model produces unrealistically high amplitudes. The basin oscillation amplitude varies on synoptic time scales (2–17 days) and exhibits seasonal variations. The optimal wind direction to generate basin-mode oscillations is along 60°/240° T. **Citation:** Xu, Y., D. R. Watts, M. Wimbush, and J.-H. Park (2007), Fundamental-mode basin oscillations in the Japan/East Sea, *Geophys. Res. Lett.*, *34*, L04605, doi:10.1029/2006GL028755.

1. Introduction

[2] The Japan/East Sea (JES) is a semi-enclosed marginal sea, whose coastal boundary largely separates it from the open ocean. The boundary prevents energy propagating away from the basin and constrains its free oscillations to discrete modes. Numerical studies [*Platzman*, 1972] have indicated that free oscillations in enclosed seas should be the normal-mode solutions for a two-dimensional basin.

[3] Observational evidence for these free oscillations in various semi-enclosed seas has come from occasional seiche episodes [*Cerovecki et al.*, 1997; *Leder and Orlic*, 2004; *Metzner et al.*, 2000]. *Rao et al.* [1976] calculated the surface normal modes of Lake Michigan and showed spectral evidence for several of the lowest modes from analyses of water level data. In the JES, *Rikiishi* [1986] studied basin-mode oscillations with a barotropic model assuming closed straits. The calculations are based on the Galerkin method developed by *Rao and Schwab* [1976] with water depth assigned on every grid after a smoothing. Rikiishi's model indicated that the fundamental basin oscillation in the JES should be a Kelvin-wave-like motion around an amphidromic point with a period of approximately 6.13 hours and a coastal wavelength equal to the circumference of the basin, as exhibited in Figure 1. The modeled mode has relatively large amplitudes in the narrow northern region and in the southwest corner of the JES.

[4] In the real JES, energy dissipation exists, four straits connect to the open ocean and bottom topography is highly variable, so Rikiishi's model may be expected to differ somewhat in period and structure from observations. We find no published report of direct observations of basin oscillations in the JES. In this paper we provide observational evidence that fundamental mode basin oscillations exist continually in the JES. The observed results are compared with Rikiishi's model, and the forcing is investigated.

2. Data and Methods

[5] Sea level, bottom pressure, and wind-stress data from the JES were analyzed. Hourly bottom pressure data came from pressure-sensor-equipped inverted echo sounders (PIESs) deployed in the southwestern JES (circles in Figure 1) for the period June 1999–July 2001 [*Mitchell et al.*, 2004]. In addition, hourly sea level data at 9 tide stations were acquired from the Korea Oceanographic Data Center and the Japan Oceanographic Data Center for the period January 1999–June 2001 (squares in Figure 1). Fourteen tide gauge sites were available which all exhibited a consistent set of amplitudes and phases in the basin-oscillations frequency band, and we have simply chosen to show a subset of nine which are well separated along the coast. One (15th) tide gauge inside a harbor between stations 4 and 5 was excluded because it had an inconsistent phase (by ~5 degrees) compared to tide station 4. We used NOGAPS Reanalysis Data of wind stress in the JES area with data interval 6 hours and grid size $1° \times 1°$. Hourly buoy wind velocity data near the Korea Strait were acquired from the Korean Meteorological Agency.

[6] Section 3.1 describes how three data analysis steps were performed sequentially to reveal the evidence of basin-mode oscillations in the JES. Power spectral analysis on the time series of sea level data and bottom pressure data identified the frequency band of the basin oscillation. These basin-mode oscillations were then isolated using a narrow 4th-order band-pass Butterworth filter. Complex empirical orthogonal function (CEOF) analysis of the band-pass-filtered data revealed the coherent basin-wide nature of these oscillations and determined their spatial structure and phase propagation.

[7] In an effort to investigate the energy sources of the basin oscillations, we have examined hourly Korea Strait transport, seismic activity around the JES, and wind forcing. There was no significant coherence with Korea Strait transport in the basin-mode frequency band [*Xu*, 2006]. We found no clear consistency between bursts of basin-mode oscillations and seismic events [*Xu*, 2006].

3. Results and Discussions

3.1. Evidence of Basin-Mode Oscillations

[8] Figure 2 shows power spectra for time series measurements of sea level at tide station 9 and of bottom pressure

[1]Institute for Geophysics, University of Texas at Austin, Austin, Texas, USA.
[2]Graduate School of Oceanography, University of Rhode Island, Narragansett, Rhode Island, USA.

0094-8276/07/2006GL028755

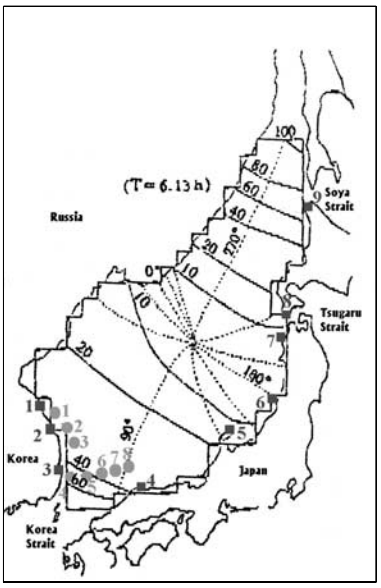

Figure 1. Fundamental-mode basin oscillation in the Japan/East Sea taken from the *Rikiishi* [1986] model. Solid lines and broken lines indicate respectively the surface elevation and phase of the fundamental-mode oscillation. Also shown are tide gauge stations (squares) and PIES sites (circles).

at PIES site 3, respectively in the northeastern and southwestern JES. Both sites exhibit enhanced energy (nearly ten times background level) for frequencies between the tidal peaks M3 and M4 (i.e., periods 6.42–7.75 hours), with a peak at 6.7 hours. This non-tidal enhanced energy has a period close to that of the fundamental basin mode modeled by *Rikiishi* [1986]. We show below that the amplitude and phase propagation of signals in this frequency band correspond to a fundamental basin mode. We also examined the peaks (around 0.21 cph and 0.24 cph) near the period (4.51 hours) of the second mode [*Rikiishi*, 1986], and did not find the corresponding phase rotation. The complication might arise from two factors (1) the signal of the second mode is small (2) the southern node of the second mode is close to the wide open Korea Strait. We identify the band (i.e., periods 6.42–7.75 hours) with the fundamental basin-mode oscillations, band-pass filter the tide gauge and PIES data within 6.42–7.75 hours, and proceed now to examine the properties in detail.

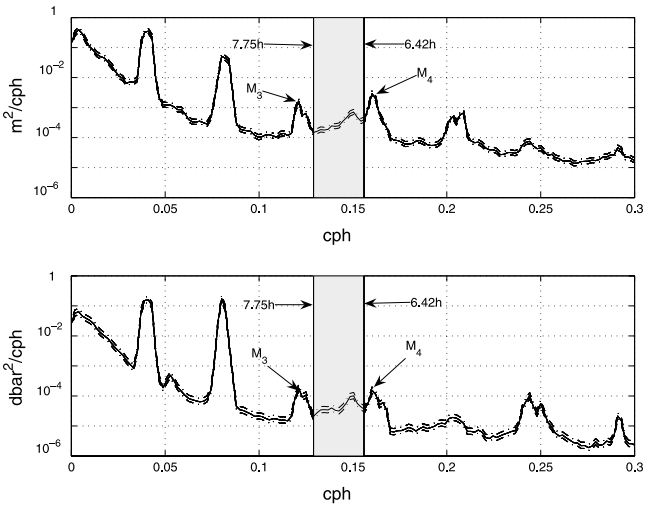

Figure 2. (top) Power spectral density of sea level at tide station 9 and (bottom) bottom pressure at PIES site 3. In the highlighted frequency band of fundamental basin oscillations, between neighboring tidal-harmonic peaks M_3 and M_4, the power level is nearly a factor of ten higher than the background. Dashed lines indicate the 95% confidence intervals determined using the inverse of chi-square cumulative distribution function [*Kay*, 1988].

[9] The CEOF eigenvectors represent the relative amplitudes and phases of the fluctuations [*Emery and Thomson*, 2001; *Katz*, 1997]. Figures 3a and 3b show the eigenvectors of the first CEOF, accounting respectively for 41% and 89% of the sea level and bottom pressure variances in the 6.47–7.75 hour band. There are at least four processes that could account for the lower percentage contribution (41%) to the tide-gauge variances: local harbor wind setup, coastal-trapped waves, local baroclinic (steric) signals, and isostatic sea level response to atmospheric pressure change within this frequency band.

[10] In Figure 3, CEOF eigenvectors rotate systematically through the numbered sites, corresponding to counterclockwise phase progression in the JES through the coastal tide stations (Figure 3a) and PIES sites (Figure 3b). In Figure 3a, the phase rotates approximately 180 degrees from

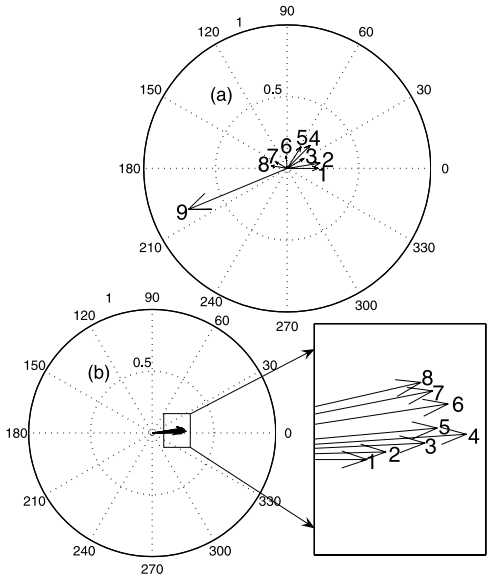

Figure 3. Amplitudes and phase progression of the fundamental mode basin oscillations indicated by eigenvectors from the first CEOF of the band-pass filtered data (6.42–7.75 hours). Vector direction and length represent respectively the relative phase lag and the amplitude. Plots are for (a) tide stations and (b) PIES sites, and account for 41% and 89% of their respective variances in the 6.42–7.75 hour band. The dimensional amplitude (mm) of the envelope of basin oscillations at a given time and location is the product of the above non-dimensional vector magnitude and the time series amplitude in Figure 4.

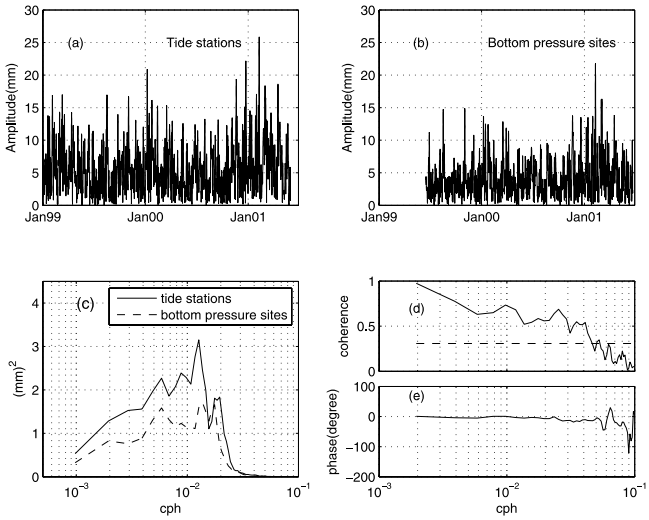

Figure 4. Temporal variability of basin oscillation amplitudes from tide station and bottom pressure site measurements. The greatest variances occur at frequencies 0.02–0.0025 cycle/hour, i.e., periods 2–17 days. Time series of the first CEOF mode of (a) tide station data and (b) bottom pressure data, band-pass filtered between periods 6.42 and 7.75 hours. (c) Variance - preserving spectra of Figures 4a and 4b. (d) Coherence and (e) phase of Figures 4a and 4b. The horizontal dashed line in Figure 4d indicates the 95% confidence level of coherence. The dimensional amplitude (mm) of the envelope of basin oscillations is given by the product of these time series and the non-dimensional vector magnitude amplitude in Figure 3 for a given site.

tide stations 1 to 8, and the corresponding along-coast distance is about half the basin circumference. This indicates that the coastal wavelength of the oscillation is just the circumference of the basin. The phase rotation among the PIES sites is small because the area coverage of the PIES sites is small. The phase rotation in the *Rikiishi* [1986] model is also small through the PIES area, and the observed and modeled phases agree well.

[11] In Figure 3a, the first CEOF relative amplitudes exhibit geographic variability that also resembles the *Rikiishi* [1986] model. Both Figure 3a and Figure 1 show large amplitudes at tide station 9. The observed (modeled) amplitudes decrease by a factor of 9 (7) from tide station 9 to tide station 7, and then increase by a factor of 2 (2) from tide station 7 to tide station 5. For tide stations 1-4, the observed relative amplitudes are smaller than Rikiishi's model results. This is presumably an artifact of the Rikiishi model, which treats the Korea Strait as closed. In the real JES, there will be partial transmission and energy leakage through this wide strait. Hence, the closed boundary in the numerical model probably accounts for its overestimation of basin-oscillation amplitudes near the strait. Figures 4a and 4b respectively show time series of the first CEOF from the coastal tide stations and the bottom pressure recorders. The two time series of the amplitude modulation (envelope) of the basin-mode oscillations exhibit bursts of high variance at similar intervals of 2–17 days. These bursts have higher amplitude in the three winters than in the two summers. Figures 4c, 4d, and 4e exhibit their corresponding variance-preserving spectra, coherence and phase for the overlap period (June 1999–June 2001). The two time series exhibit high energy at atmospheric synoptic time scales of 2–17 days. Their mutual coherence at periods longer than 1 day is significant, with phase close to zero. All of this suggests strongly that the sea-level and bottom-pressure measurements observe the same basin mode.

3.2. Energy Sources of Basin-Mode Oscillations

[12] The fundamental basin oscillations in the JES are a free mode. Their basin-wide nature allows non-local response to a variety of mechanisms that force water motions, including changes in the wind or atmospheric pressure gradient. The non-local response to multiple forcings can therefore lead to an unsteady phase relationship, and hence incoherence, with any one specific or local forcing process. We found no significant coherence in the basin-oscillation frequency band between hourly wind speed in the Korea Strait and the pressure record from PIES site 6. We next examined the joint variability of basin-scale wind forcing and basin oscillations utilizing cross wavelet analysis [*Grinsted et al.*, 2004], which is well suited to reveal joint variability in two processes regardless of their phase coherence.

[13] Figure 5 exhibits the cross wavelet power between the time series of the first tide-station-data CEOF and the basin-averaged east-west wind stress. Cross wavelet power (of two time series, $x(t)$ = basin mode amplitude and $y(t)$ = wind stress) is estimated as the complex modulus $\sum |W_x W_y^*|$ of the product of their Morlet wavelet transforms in the frequency-time domain, which are the convolutions of the Morlet wavelet function with the original time series [*Torrence and Compo*, 1998]. The cross wavelet power indicates the strength of the joint variability as a function of frequency and time. Events of statistically significant common power are observed throughout the 2–17 day band, and their time dependence reflects the

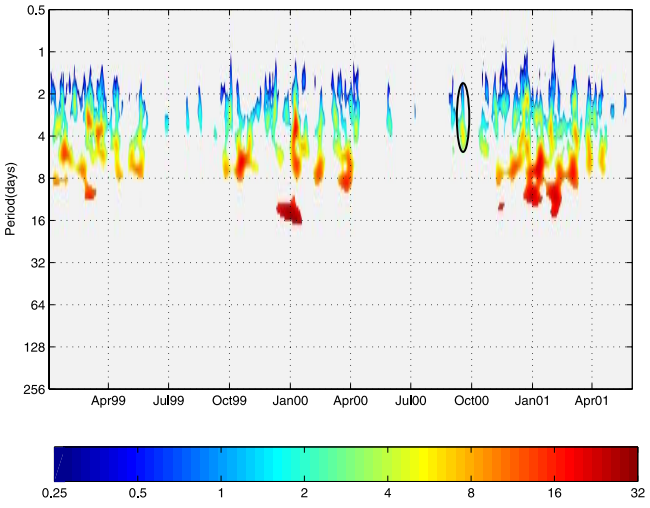

Figure 5. Cross wavelet power between the time series of the first CEOF of tide station data and the basin averaged east-west wind stress. Only the values above 95% confidence level are shown. Basin oscillations and wind stress vary jointly at periods 2–17 days. The circled spot corresponds to the passing of Typhoon Saomai across the Japan/East Sea on September 15–16, 2000.

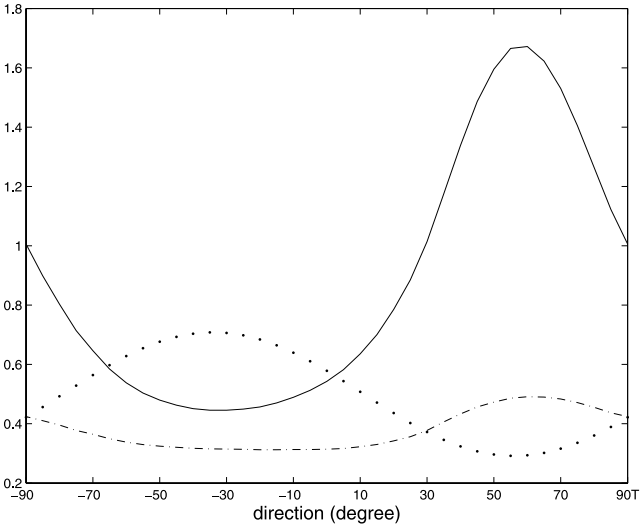

Figure 6. Wind stress variance Var_y (dotted line) normalized by the variance of the total wind stress, sum of the significant cross wavelet power $\sum |W_x W_y^*|$ (dot-dashed line) between the time series of basin-mode amplitude $x(t)$ and the wind stress $y(t)$ normalized by the total time-frequency area of significant cross wavelet power, and effectiveness of wind stress to generate basin oscillations $\frac{\sum |W_x W_y^*|}{Var_y}$ (solid line) as a function of wind direction. The wind stress at 60°T is most effective at generating basin oscillations. The normalizations used allow all three curves to be plotted together on one non-dimensional ordinate.

episodic character of the basin oscillations and the wind events. Moreover, Figure 5 exhibits a clear seasonal variation of enhanced common power, highest between October and April. The circled event highlights one strongest typhoon that passed through the JES during this two year period [*Park and Watts*, 2005].

[14] To investigate whether basin oscillation amplitudes depend on the direction of the wind stress in the JES, we calculate the cross wavelet power between the time series of the first CEOF and the wind stress in a suite of directions at 5 degree interval around the compass. Each time series was divided by its standard deviation prior to convolution with the Morlet wavelet to focus on the variability of the data. We calculate the ratio $\frac{\sum |W_x W_y^*|}{Var_y}$ where $\sum |W_x W_y^*|$ is the sum of the significant cross wavelet power in Figure 5, and Var_y is the variance of the basin-averaged wind stress in a particular direction. This ratio represents the relative effectiveness of wind stress in different directions for generating basin oscillations. Figure 6 shows that wind-stress oriented near 60°T produces the largest amplitude basin oscillations, even though the wind stress itself is twice as large in the orthogonal direction along −30°T (i.e. 330°T). The direction 60°T is turned somewhat clockwise from the major axis of the JES (∼30°T) along which wind stress would act with greatest fetch. We speculate that the turning arises from a combination of two atmospheric forcing processes that can affect sea level difference from the southern to northern end of the JES: the above noted wind stress and the atmospheric pressure difference. Zonal winds are associated with meridional atmospheric pressure gradients, which would add to the sea-level set up that is directly forced by wind stress. Consequently, a response to meridional atmospheric pressure gradient may account for the zonal turning from the longest fetch direction (30°T) into the observed optimal direction (60°T). Because the wind and atmospheric pressure are highly correlated, their effects are not easily distinguished statistically. We suggest that a future numerical model study might consider the wind stress and atmospheric pressure forcing separately to test this hypothesis for the JES.

4. Conclusion

[15] We present the first observational evidence that basin oscillations are frequently excited in the JES. The fundamental-mode basin oscillation, influenced by the Earth's rotation, consists of a single amphidromic point around which the wave propagates counter-clockwise. It has a period of about 6.7 hours and a coastal wavelength equal to the circumference of the JES.

[16] Both tide-station and bottom-pressure data confirm counterclockwise phase rotation in the frequency band of the fundamental basin mode in the JES. The relative amplitudes support the spatial structure of the Rikiishi model, except at stations near the Korea Strait where the model assumed a closed boundary and hence obtained artificially large amplitudes.

[17] The observed basin-oscillation amplitude varies on synoptic time scales (2–17 days) and exhibits both seasonal and interannual variations. The observed optimal direction of wind stress to generate basin-mode oscillation is along 60°/240°T, which we tentatively attribute to the geographic shape of the JES.

[18] The basin-oscillation amplitude is the product of its CEOF spatial amplitude and the time component. This amplitude can reach 2–3 cm for tide station 9 and 0.2–0.4 cm for other tide stations in the JES. These high frequency signals will cause aliasing errors in satellite altimeter observations, especially in the narrow northern region. Aliasing effects arising from the basin-mode oscillations can be removed from satellite data using tide station or bottom pressure measurements.

[19] **Acknowledgments.** We thank two anonymous reviewers for their helpful comments. We thank Karen Tracey for her help in processing the bottom pressure data. We thank Korea Oceanographic Data Center and Japan Oceanographic Data Center for their coastal tide gauge data. William J. Teague kindly provided us with NOGAPS atmospheric data. We also thank Tae-Hee Kim, Jiyoung Kim and John Merill for their help in acquiring hourly wind data. This work was supported by the Office of Naval Research grant N000140410658.

References

Cerovecki, I., M. Orlic, and M. C. Hendershott (1997), Adriatic seiche decay and energy loss to the Mediterranean, *Deep Sea Res., Part I*, *44*, 2007–2029.

Emery, W. J., R. E. Thomson (2001), *Data Analysis Methods in Physical Oceanography*, 2nd ed., 638 pp., Elsevier, New York.

Grinsted, A., J. C. Moore, and S. Jevrejeva (2004), Application of the cross wavelet transform and wavelet coherence to geophysical time series, *Nonlinear Processes Geophys.*, *11*, 561–566.

Leder, N., and M. Orlic (2004), Fundamental Adriatic seiche recorded by current meters, *Ann. Geophys.*, *22*, 1449–1464.

Katz, E. J. (1997), Waves along the equator in the Atlantic, *J. Phys. Oceanogr.*, *27*, 2536–2544.

Kay, S. M. (1988), *Modern Spectral Estimation*, 543 pp., Prentice-Hall, Upper Saddle River, N. J.

Metzner, M., M. Gade, I. Hennings, and A. B. Rabinovich (2000), The observation of seiches in the Baltic Sea using a multi data set of water levels, *J. Mar. Syst.*, *24*, 67–84.

Mitchell, D. A., Y. Xu, K. L. Tracey, D. R. Watts, M. Wimbush, and W. J. Teague (2004), PIES data report: Ulleung Basin in the Japan/East Sea, *Tech. Rep. 2004-02*, 98 pp., *Grad. Sch. of Oceanogr.*, Univ. of R. I., Narragansett.

Park, J.-H., and D. R. Watts (2005), Response of the southwestern Japan/East Sea to atmospheric pressure, *Deep Sea Res., Part II*, *52*, 1671–1683.

Platzman, G. W. (1972), Two-dimensional free oscillations in natural basins, *J. Phys. Oceanogr.*, *2*, 117–138.

Rao, D. B., and D. J. Schwab (1976), Two-dimensional normal modes in arbitrary closed basins on a rotating Earth: Application to Lake Ontario and Superior, *Philos. Trans. R. Soc. London, Ser. A*, *281*, 63–96.

Rao, D. B., C. H. Mortimer, and D. J. Schwab (1976), Surface normal modes of Lake Michigan: Calculations compared with spectra of observed water level fluctuations, *J. Phys. Oceanogr.*, *6*, 575–588.

Rikiishi, K. (1986), Tides and natural oscillations in the Japan Sea (in Japanese), *Kaiyo Monthly*, *18*, 447–454.

Torrence, C., and G. P. Compo (1998), A practical guide to wavelet analysis, *Bull. Am. Meteorol. Soc.*, *79*, 61–78.

Xu, Y. (2006), Analyses of sea surface height, bottom pressure and acoustic travel time in the Japan/East Sea, Ph.D. thesis, 86 pp., Univ. of R. I., Narragansett.

J.-H. Park, D. R. Watts, and M. Wimbush, Graduate School of Oceanography, University of Rhode Island, 215 South Ferry Road, Narragansett, RI 02882-1197, USA.

Y. Xu, Institute for Geophysics, University of Texas at Austin, Austin, TX 78759, USA. (yongsheng@utig.ig.utexas.edu)